Transcriptomics elucidates metabolic regulation and functional promoters in the basidiomycete red yeast *Xanthophyllomyces dendrorhous* CBS 6938

Emma E. Tobin[1,†], Joseph H. Collins[1,†], Celeste B. Marsan[1], Gillian T. Nadeau[1], Kim Mori[1], Anna Lipzen[2], Stephen Mondo[2], Igor V. Grigoriev[2,3], Eric M. Young[1]*

[1] Life Sciences and Bioengineering Center, Department of Chemical Engineering, Worcester Polytechnic Institute, Worcester, MA

[2] U.S. Department of Energy Joint Genome Institute, Lawrence Berkeley National Laboratory, Berkeley, CA 94720

[3] Plant and Microbial Biology, University of California Berkeley, Berkeley, CA 94720

[†] Equal contribution

* To whom correspondence should be addressed. emyoung@wpi.edu

ABSTRACT

Genomics has become the primary way to explore microbial diversity, because genetic tools are currently difficult to develop in non-model organisms. Here, we demonstrate that -omics can be leveraged to accelerate genetic tool development for the basidiomycete yeast *Xanthophyllomyces dendrorhous* CBS 6938, the sole biotechnologically relevant organism in the Tremellomycete family. First, we sequence the genome. Then, we perform transcriptomics under a variety of conditions, focusing on light and oxidative stress. This data not only reveals novel photobiology and metabolic regulation, it also allows derivation of constitutive and regulated gene expression parts. Our analysis of *X. dendrorhous* photobiology shows for the first time that a complex system of white-collar and cryptochrome homologs mediate response to ultraviolet light (UV). Our analysis of metabolic regulation shows that UV activates DNA repair, aromatic amino acid and carotenoid biosynthesis and represses central carbon metabolism and the fungal-like apoptotic pathway. Thus, *X. dendrorhous* shows a dynamic response toward biosynthetic pathways for light-absorbing compounds and survival and away from energy production. We then define a modular cloning system, including antibiotic selections, integration sites, and reporter genes, and use the transcriptomics to derive strong constitutive and regulated promoters. Notably, we discover a novel promoter from a hypothetical gene that has 9-fold activation upon UV exposure. Thus, -omics-to-parts workflows can simultaneously provide useful genomic data and advance genetic tools for non-model microbes, particularly those without a closely related model organism. This approach will be broadly useful in current efforts to engineer diverse microbes.

INTRODUCTION

Yeasts are a diverse group of fungi characterized by unicellular growth, which is useful in industrial fermentations. The group is not monophyletic, rather the yeast state has emerged several times across the fungal kingdom. Therefore, yeasts have vastly different genome architectures, metabolic capabilities, and stress tolerances that are not only due to the ecological niches to which they are adapted, but also due to their different lineages. The impact this biodiversity might have on industrial biotechnology has only just begun to be explored.[1] However, the different lineages limit the transferability of genomics and genetic tools between yeasts, particularly for the basidiomycete yeasts that are not closely related to any model organism.[2] Here, we demonstrate how modern genomics and transcriptomics can be leveraged to simultaneously gain new insight into nonconventional yeast biology and derive a collection of genetic parts for future studies. We demonstrate this for the basidiomycete yeast *Xanthophyllomyces dendrorhous,* the only biotechnologically relevant organism from the Tremellomycete family of Basidiomycota.[3]

Historically, the model ascomycete *Saccharomyces cerevisiae* has been the host of choice for yeast metabolic engineering.[4] While valuable for converting hexoses to ethanol, engineering *S. cerevisiae* to consume other carbon sources and produce other economically valuable compounds can require extensive reprogramming, which imposes metabolic and gene expression burden.[5] This is particularly true of tolerance, which can be due to many genes interacting in currently unpredictable ways. This has led to a growing body of literature that investigates other yeasts, termed nonconventional simply because they are not *S. cerevisiae*, as potential hosts for metabolic engineering since they are already adapted to consume desired carbon sources, produce desired classes of molecules, and tolerate different fermentation conditions, thus less burden is incurred when engineering them.[6,7] Methods for developing genetic tools are needed for these organisms.

46 Developing genomics and genetic tools in nonconventional yeasts is challenging. This is
47 because a high-quality genome, gene regulatory data, species-specific DNA parts for genetic
48 manipulation, and efficient transformation procedures are often missing. The process of
49 developing these elements, termed "onboarding," can be accelerated for nonconventional
50 ascomycete yeasts closely related to *S. cerevisiae* because the genomics and genetics are
51 similar, permitting transfer of similar promoter and plasmid designs. Onboarding organisms from
52 relatively unknown classes, particularly basidiomycete yeasts, does not have this advantage
53 because there is not a closely related model organism with a complete, contiguous genome and
54 well-developed genetics.

55 *Xanthophyllomyces dendrorhous* is a nonconventional yeast that has gained attention in
56 the aquaculture and nutraceutical industries due to its natural ability to produce astaxanthin, a
57 vibrant red pigment with potent antioxidant properties. It is currently the only Tremellomycete with
58 biotechnology applications. While gene knock-out and upregulation techniques have been
59 employed to modify *X. dendrorhous,* particularly strain CBS 6938, reprogramming this yeast
60 remains a challenge because several key tools in the onboarding toolkit are missing, including a
61 high-quality genome sequence, a modular gene expression parts collection, and efficient
62 transformation methods.[6] Furthermore, astaxanthin is only overproduced in response to light and
63 oxidative stress, which complicates and limits the scale of bioprocesses.[7–9]

64 Here, we demonstrate an omics-driven onboarding workflow including genome
65 sequencing, transcriptomics, high efficiency transformation, and modular gene expression parts
66 collection development for *X. dendrorhous*. This workflow generates new insights into
67 basidiomycete photobiology and metabolism, constitutive promoters, light-inducible promoters,
68 and efficient genome integration. Therefore, this "omics-to-parts" approach can rapidly deliver a
69 suite of data and tools for onboarding nonconventional yeast that have no closely related model
70 host.

71 **RESULTS**

72 **High quality genome of *X. dendrorhous* CBS 6938**

73 A high-quality CBS 6938 genome was obtained through Prymetime sequencing (Figure
74 1a).[10] Prymetime assembled the genome into sixteen contigs, and relative lengths of the contigs
75 are depicted in the figure. Subsequent benchmarking universal single-copy ortholog (BUSCO)
76 analysis revealed that the CBS 6938 genome contains 94.0% complete and single copy BUSCOs
77 (Figure 1b). This genome sequence was the foundation for the subsequent work.

78 **Foundational genetic tools for onboarding *X. dendrorhous***

79 In addition to obtaining an accurate genome sequence, we performed a set of experiments
80 to make *X. dendrorhous* easier to engineer. We first examined possible selection markers. Rather
81 than seek to create synthetic auxotrophy, which has a variety of metabolic impacts,[11] we screened
82 for antibiotic sensitivity. We measured *X. dendrorhous* sensitivity to several common antifungals
83 via minimum inhibitory concentration (MIC) assay (Methods). The most effective antifungal was
84 found to be nourseothricin with 11.6% cell survival at a concentration of 10 µg/mL (Figure 2a).

85 We then designed a modular cloning system for rapidly assembling *X. dendrorhous*
86 genetic elements (Figure 2b). This system uses the same enzymes and scars as previously
87 published modular cloning systems.[12] There are two significant differences in this red yeast
88 modular cloning system. The first is that the *lacZ* element in the destination plasmids is replaced
89 with the lethal gene *ccdb* to shift from blue/white screening of correct clones to a system where
90 only correct clones are able to grow on a selection plate. The second is that the Level 2 (L2)
91 integrative plasmid has homology arms compatible with the *X. dendrorhous* genome. We used
92 our genome sequence to select homology arms flanking that *crtYB* gene, the gene that catalyzes

93 production of the colorful carotenoid pigments. This creates a facile red/white screening method
94 for correctly integrated clones.

95 We then designed an initial integration cassette using the known glutamate
96 dehydrogenase promoter (P_{gdh}) to drive expression of a codon-optimized *nat* gene which confers
97 nourseothricin resistance. We used this initial integration cassette to optimize the efficiency of
98 transformation. The method we found to be most efficient is described in Methods. In brief, it
99 consists of the culture of CBS 6938 cells until the end of exponential growth phase is reached,
100 combination with the integrative pathway, and application of an electric shock (Figure 2c). Ultra-
101 high-performance liquid-chromatography (UPLC) was then used to demonstrate successful *crtYB*
102 knock-out through measurement of astaxanthin. Astaxanthin peaks were detected in wild type but
103 not knock-out extractions (Figure 2d). Thus, with the design of the integration cassette and
104 optimization of the transformation protocol we are able to achieve efficient and targeted
105 integration of DNA into the *X. dendrorhous* genome using homologous recombination.

106 We then established a luminescent reporter, which is common in fungal engineering, for
107 measuring gene expression strength. We cloned the NanoLuc enzyme[13] into our modular cloning
108 scheme, integrated it into the genome, and measured expression via luciferase assay (Figure 2e).
109 NanoLuc-producing cells created approximately 1,000-fold greater luminescence compared to
110 the *crtYB* knockout strain, and nearly 10,000-fold greater luminescence compared to CBS 6938.
111 The higher luminescence observed from the *crtYB* knockout strain may be attributed to biological
112 autoluminescence, a phenomenon that has been found to be directly related to oxidative stress.[14]

113 Together with the genome sequence, these experiments enabled the development of
114 advanced genetic tools for *X. dendrorhous*.

115

116 **Confirming that astaxanthin biosynthesis responds to light through transcriptional**
117 **regulation**

118 We next sought to more fully understand *X. dendrorhous* biology by examining genetic
119 response to light and oxidative stress. While previous work has shown that visible and ultraviolet
120 (UV) light increases carotenogenesis in *X. dendrorhous*, specific genes and mechanisms involved
121 in this regulation have not been investigated. Therefore, we first sought to confirm that the
122 carotenogenesis pathway was transcriptionally regulated. Before conducting transcriptomics, we
123 used the genome sequence to design quantitative polymerase chain reaction (qPCR) probes to
124 target genes in the terpenoid (*MVK*, *PMVK*, *MVD*, *IDI*, *FPS*, and *crtE*) and carotenogenic (*crtYB*,
125 *crtI*, and *crtS*) pathways. Cells were grown under either dark or UV-light conditions, RT-qPCR
126 was performed, and log2 fold-change was calculated (Methods). Upstream genes *MVK*, *PMVK*,
127 *MVD*, *IDI*, *FPS*, and *crtE* exhibited little to no expression response. However, *crtYB*, *crtI*, and *crtS*
128 expression was upregulated by UV light exposure. Notably, the *crtI* gene was the most impacted
129 with log2 fold-changes of 0.90 (Figure 3a). These results demonstrate that light, particularly UV,
130 transcriptionally upregulates carotenogenesis, not the upstream terpenoid pathway, in *X.*
131 *dendrorhous*.

132

133 **Transcriptomics to elucidate *X. dendrorhous* photobiology**

134 We then designed a transcriptomics experiment to investigate the genome-wide response
135 of *X. dendrorhous* across the light spectrum including UV, blue, green, and red light. We included
136 a positive control condition of oxidative stress by hydrogen peroxide exposure, and growth of cells
137 in the dark was used as a negative control (Methods) (Figure 4a). We extracted the RNA, which
138 was then sequenced and processed by the DOE Joint Genome Institute through their Community
139 Science Program. We defined a noteworthy log2 fold-change as any greater than 0.50.

140 The data corroborated our previous evidence that exposure to UV light leads to
141 upregulated expression of crtI with a log2 fold-change of 0.90. Further, the upstream terpenoid
142 pathway again had no significant changes, indicating upstream terpenoid synthesis to the
143 diterpenoid intermediate, geranylgeranyl pyrophosphate, was unaffected by light. In contrast,
144 oxidative stress upregulated genes in both pathways (*MVK*, *PMVK*, *IDI*, *FPS*, *crtYB*, and *crtI*),
145 with *IDI* having the greatest increase (log2 fold-change of 1.79) (Figure 4b). Induction of oxidative
146 stress may be a method to overcome the bottleneck that *IDI* imposes on the mevalonate
147 pathway.[15] Overall, the results corroborate the previous evidence that UV light upregulates the
148 final three steps of carotenogenesis in *X. dendrorhous* and show that oxidative stress broadly
149 upregulates terpenoid biosynthesis.

150 We then looked for possible light response systems in *X. dendrorhous.* There are several
151 known classes of fungal light receptors, particularly white collar and cryptochrome proteins in
152 ascomycete and two receptors in basidiomycetes, BLUF, which senses to blue light, and
153 rhodopsin, which senses green light.[16] We searched our *X. dendrorhous* CBS 6938 genome with
154 BLAST for putative fungal photoreceptor proteins within the BLUF, rhodopsin, white collar, and
155 cryptochrome families. Photoreceptor proteins predicted to be in the same family were
156 differentiated with arbitrarily assigned numbers. We found that the putative cryptochromes
157 increased transcription most dramatically in UV and blue light exposure. To our knowledge, this
158 is the first evidence of cryptochrome light response systems in basidiomycetes. Additionally,
159 putative white collar and rhodopsin genes increased expression. Analysis of the oxidative stress
160 positive control corroborated that these genes were responding specifically to light because most
161 putative photoreceptors were downregulated or unaffected by hydrogen peroxide (Figure 4c).

162 Finally, we filtered the whole genome transcriptomic data for the genes most up- or
163 downregulated by UV light. We identified ten upregulated and six downregulated genes with log2
164 fold-changes of 1.50 or greater (Figure 4d). These genes were from different functional classes,

165 from cell survival to energy storage. Endonuclease III, MSS4-like protein, and short-chain
166 dehydrogenases are directly involved in response to UV stress through DNA repair, cell survival
167 through cell cycle regulation and actin cytoskeleton formation, and induction of light-regulated
168 pathways, respectively.[17–19] These functions collectively correspond to an expected stress
169 response from UV exposure.[20] Conidiation-specific protein 6, a protein involved in the
170 reproductive cycle, is also upregulated after blue-light exposure in *Neurospora crassa*.[21]
171 Unexpectedly, UV light upregulates expression of glycogenin glucosyltransferase, an enzyme that
172 initiates glycogen nucleation. Downregulated genes were found to be involved in transcriptional
173 regulation, fungal apoptotic-like cell death, and the electron transport chain. Also of note, four of
174 the ten upregulated genes were predicted to result in hypothetical proteins, indicating that our
175 understanding of light response mechanisms is incomplete. Genes most up- or downregulated in
176 response to hydrogen peroxide exposure were found to not be affected by light treatments, further
177 supporting the notion of separate response pathways (Figure 4e). In summary, it appears that *X.*
178 *dendrorhous* activates DNA repair, survival, and reproductive mechanisms while downregulating
179 programmed cell death. The metabolic response is complex, with some pathways upregulated
180 and others downregulated.

181 To more clearly analyze the metabolic response, genes were clustered into functional
182 groups using the ERGO™ Bioinformatics platform from Igenbio. Upregulation of functional groups
183 is depicted in Figure 5a. Generally, DNA repair and amino acid metabolic functions were
184 upregulated. Interestingly, aromatic amino acid degradation and modification were upregulated
185 by both UV light and hydrogen peroxide, but amino acid uptake was only upregulated in UV-
186 exposed cells. Furthermore, electron transport, glycolysis, gluconeogenesis, and carbohydrate
187 metabolism were downregulated (Figure 5b). These results support the general trends observed
188 in the analysis of individual genes. We synthesized all of these observations into a qualitative
189 description of the CBS 6938 metabolic shift in response to UV (Figure 5c). With this view, the

190 transcriptional response indicates that *X. dendrorhous* likely redirects flux from central carbon
191 metabolism to carotenoids and aromatic amino acids upon UV exposure. Aromatic amino acids
192 absorb UV and are also precursors to other UV light absorbing molecules like melanin and
193 mycosporine compounds.[22–24] Yet, the activation of aromatic amino acid pathways in response to
194 UV has not been previously observed in basidiomycetes. These results indicate that the response
195 to UV in *X. dendrorhous* is more extensive and complex than acting on carotenogenesis alone.
196 Furthermore, the significant fraction of hypothetical proteins hints at additional unknown
197 mechanisms that also contribute to the response to UV exposure.

198 **Transcriptomics-driven part selection allows simultaneous derivation of constitutive and**
199 **regulated genetic parts**

200 We then leveraged the transcriptomics data to derive functional genetic elements for use
201 in our established modular cloning scheme. Since the data covered a variety of conditions, we
202 reasoned that it should be possible to derive putative constitutive and regulated promoters. We
203 identified strong constitutive promoters by sorting each transcriptomics dataset by fragments per
204 kilobase of exon per million mapped fragments (FPKM) count, choosing the genes that had the
205 highest and consistent FPKM counts across conditions (Figure 6a), and using our genome
206 sequence to obtain the sequences upstream of those genes. We also obtained the sequences
207 upstream of the genes in Figure 4c that were the most activated or repressed by UV light (Figure
208 6a). Promoter lengths were chosen with the assistance of an analysis conducted by JGI. These
209 putative promoters were then cloned into our modular cloning system to drive expression of
210 nanoluciferase and integrated into the genome (Figure 6b).

211 We measured expression of each construct via a luciferase assay in the dark and under
212 UV exposure (Methods). As Figure 6c shows, the constitutive promoters result in high
213 luminescence that does not change between the dark and the light. In contrast, the putative UV

214 activated promoters showed increased luminescence in response to UV (Figure 6c). However,
215 most of these increases were not large. The two strongest inducible promoters were found to be
216 hypothetical proteins HP3 and HP2 with log2 fold-changes of 3.01 and 1.47, respectively. This
217 means that the strongest UV-inducible promoter results in a 9-fold change in gene expression.
218 The putative UV repressed promoters did not show any significant repression. We reasoned that
219 the long half-life of luciferase was confounding measurement of repression. Thus, we designed a
220 qPCR experiment, and the results indicated no change. Therefore, it is possible our promoter
221 lengths were insufficient to capture the regulatory elements in these promoters.

222 Taken together, our results show that transcriptomics driven part discovery can
223 consistently derive strong constitutive promoters, but inconsistently derive regulated promoters
224 due to a variety of possible factors. Even so, we were able to discover two promoters that can be
225 activated by UV. Thus, our part discovery efforts generated a collection of constitutive and
226 regulated promoters that are compatible with our modular cloning workflow for *X. dendrorhous*
227 CBS 6938.

228 **DISCUSSION**

229 In this study, a promising nonconventional yeast was subjected to a streamlined set of
230 genomics and genetics experiments that transformed it into a powerful platform for genetic
231 engineering. This was done by obtaining a high-quality genome, increasing transformation
232 efficiency, developing advanced modular genetic tools, measuring gene regulation, and deriving
233 a genetic parts collection from transcriptomic data. Now, it is possible to interrogate the unique
234 metabolism and photobiology of *X. dendrorhous* in a similar manner to other nonconventional
235 yeasts.

236 Our analysis of *X. dendrorhous* photobiology revealed a number of novel insights into the
237 biological mechanisms of basidiomycete light response. We found evidence of multiple different

238 fungal light response systems, including the first indication of cryptochromes in basidiomycetes.
239 We determined for the first time that light transcriptionally regulates the carotenoid, or
240 tetraterpenoid, pathway but not the upstream terpenoid pathway. We learned that *X. dendrorhous*
241 engages a variety of survival responses in response to UV, including activation of DNA repair and
242 reproduction pathways and repression of the fungal apoptotic-like pathway. We also observed a
243 complex transcriptional response in metabolism, where central carbon metabolism is repressed
244 in favor of aromatic amino acid and tetraterpenoid biosynthesis. Taken together, these data paint
245 a picture of an extensive and coordinated response to light. This complex system is likely key to
246 survival of *X. dendrorhous* in its ecological niche of fallen trees at high altitudes, which would
247 include extended periods of intense UV exposure.

248 It is interesting to note that our genome integration approach results in efficient on-target
249 insertion of constructs via homologous recombination (HR). Our findings support the results of
250 others that *X. dendrorhous* CBS 6938 has an active HR pathway, which is incredibly beneficial
251 for future strain engineering efforts. This challenges the dogma that nonconventional yeasts favor
252 the non-homologous end joining (NHEJ) mechanism, and argues that other yeasts besides *S.*
253 *cerevisiae* favor HR.[25,26]

254 Leveraging transcriptomics allowed us to derive constitutive and regulated gene
255 expression parts. Transcriptomics has been previously used to identify regulated promoters in
256 other yeasts. We built on this prior evidence and coupled it with a modular cloning standard to
257 create an -omics-to-parts workflow that can yield needed constitutive and inducible promoters for
258 construction of genetic devices. This -omics-to-parts workflow can be generalized to derive
259 genetic parts collections for a number of nonconventional microbes.

260 Development of novel production platform hosts requires an understanding of genome
261 composition and genetic regulation, which also is essential for genetic tool and genetic part
262 development. This work demonstrates how an integrated genomics and genetics approach can

263 simultaneously deliver new biological understanding and onboard a nonconventional organism,
264 particularly a nonconventional yeast with no closely related model organism. This integrated
265 approach, consisting of a small number of experiments, promises to accelerate organism
266 onboarding efforts.

267

268

269 **MATERIAL AND METHODS**

270 **Strains and media**

271 The *X. dendrorhous* type strain CBS 6938 (ATCC 96594) was cultured at 21 °C in YPD
272 (YEP, Sunrise Science, 1877-1KG plus 20 g/L glucose, Alfa Aesar, A16828) media for all
273 experiments. For all light plate apparatus experiments, the *X. dendrorhous* seed cultures were
274 shielded from any external light by wrapping the flasks with aluminium foil. *X. dendrorhou*s
275 transformants were selected using YPD with 30 mg/L nourseothricin (Jena Bioscience, AB-101-
276 10ML). Solid media plates were made using 20 g/L agar (Sunrise Science, 1910-1KG). Golden
277 gate (Type-IIS) cloning was conducted using chemically competent *Escherichia coli* DH5α cells
278 (NEB, C2987H). Construction of destination vectors with the toxic selection marker ccdB was
279 done with chemically competent One Shot ccdB Survival 2 T1R *E. coli* cells (Invitrogen, A10460).
280 Both *E. coli* strains were grown in 25 g/L LB Miller broth (Fisher Scientific, BP1426-2) at 37°C.
281 Antibiotic selection was carried out using 100 mg/L carbenicillin (Alfa Aesar, J61949), 25 mg/L
282 chloramphenicol (Alfa Aesar, B20841), and 50 mg/L kanamycin (Alfa Aesar, J61272) for level 0,
283 level 1, and level 2 assemblies, respectively.

284 **gDNA isolation and sequencing**

285 Isolation of gDNA from *X. dendrorhous* and next-generation sequencing was performed
286 as described by Collins et al.[10]

287 **Construction of a light plate apparatus for various light wavelengths**

288 The light plate apparatus (LPA) was assembled following a user's manual published by
289 the Tabor lab at Rice University.[27] The LPA is an instrument capable of shining two individual LED
290 lights on cell cultures in a 24-well plate. It is comprised of a 3D-printed shell surrounding a

291 soldering board with 48 LED light sockets oriented below a 24-well plate with a clear bottom
292 (AWLS-324042, Arctic White). The LPA allows each culture to be exposed to two unique LED
293 lights without disrupting neighboring cultures.

294 **RNA isolation from the light plate apparatus**

295 LPA cultures were started in 2 mL of YPD media at OD_{600} = 1 and shaken for 4 hours at
296 200 rpm while exposed to one red (λ = 660 nm), green (λ = 565 nm), blue (λ = 470 nm), white
297 (visible light spectrum), or UV LED light (λ = 400 nm), or no LED light. For the transcriptome
298 sequencing experiments, the hydrogen peroxide condition replaced the white light condition. The
299 hydrogen peroxide condition consisted of YPD media with hydrogen peroxide at a concentration
300 of 10 mM and had no LED light. 1 mL of *X. dendrorhous* culture was taken forward for RNA
301 isolation, which used a cell homogenization and TRIzol-based method. *X. dendrorhous* cells were
302 first resuspended in 200 µL of cell lysis buffer (0.5 M sodium acetate, 5% SDS, 1 mM EDTA) and
303 transferred to pre-filled tubes with 400-micron zirconium beads (OPS diagnostics, PFMB 400-
304 100-34). The cells were homogenized using a FastPrep-24 machine from MP Biomedical for two
305 cycles at 6 m/s for 30 seconds each, with a 1-minute incubation on ice between each cycle. 800
306 µL of Trizol reagent (Invitrogen, 15596026) was then added to the cell lysate and incubated on
307 ice for 10 minutes, followed by two more cycles on the FastPrep machine. On ice, 100 µL of 1–
308 bromo–3–chloropropane (Sigma Aldrich, B9673-200ML) was added to the cell lysate, inverted to
309 mix, and incubated for 5 minutes. The tubes were spun down at 4°C for 14,000 x g for 15 minutes.
310 400 µL of supernatant was transferred to 400 µL of 100% ethanol. The RNA was purified using
311 the Monarch Total RNA Miniprep Kit (NEB, T2010S) following the supplier's instructions.

312 **qRT-PCR evaluation of carotenogenesis pathway activity in response to light exposure**

313 RNA samples were converted to cDNA using the Protoscript II First Strand cDNA
314 Synthetsis Kit (NEB, E6560S) following the supplier's standard protocol instructions. RT-qPCR
315 was then performed using IDT's PrimeTime Gene Expression Master Mix (Integrated DNA
316 Technologies Inc., Skokie, Illinois, 1055772) and PrimeTime qPCR pre-mixed assay with probes
317 and primers. Sequences can be found in Supplementary Table 2. Probes targeting genes-of-
318 interest were labeled with FAM fluorophores and probes targeting the actin housekeeping gene
319 were labeled with HEX fluorophores. Primers were designed on Benchling (https://benchling.com/)
320 and optimal probe placement was determined using PrimerQuest
321 (https://www.idtdna.com/PrimerQuest). The QuantStudio 6 Flex system was used, and
322 instructions provided by IDT for the standard cycling protocol were followed.

323 **RNA transcriptome sequencing and differential gene expression analysis**

324 cDNA prep and sequencing protocol JGI method for cDNA preparation and sequencing.
325 Raw FASTQ file reads were filtered and trimmed using the Joint Genome Institute (JGI) QC
326 pipeline.[28] Filtered reads from each library were aligned to the reference genome using HISAT
327 version 0.1.4-beta.[29] featureCounts was used to generate the raw gene counts file using gff3
328 annotations.[30] Raw gene counts were used to evaluate the level of correlation between biological
329 replicates using Pearson's correlation and determine which replicates would be used in the DGE
330 analysis. DESeq2 (version 1.10.0) was subsequently used to determine which genes were
331 differentially expressed between pairs of conditions.[31] The parameter used to call a gene
332 differentially expressed between conditions was a P-value < 0.05.

333 **Gene set enrichment analysis**

334 Annotated *X. dendrorhous* CBS 6938 genome and gene count table from mapped
335 transcriptomic reads were uploaded to ERGO 2.04 (Igenbio, inc).[32] Genes were functionally
336 enriched according to ERGO groups using GAGE5.[33]

337 **Polymerase Chain Reaction (PCR)**

338 All PCRs were done using Q5 2X Master Mix (NEB, M0492L). Primers were designed on
339 Benchling (https://benchling.com/) and the NEB Tm Calculator (https://tmcalculator.neb.com/). All
340 primers were ordered from IDT. PCR reactions closely followed NEB instructions. Briefly,
341 reactions were done in 50 µL total volume; 25 µL Q5 Master Mix, 2.5 µL of each primer, X µL of
342 template DNA (1 ng plasmid DNA or 100 ng genomic DNA), and 20-X µL nuclease free water
343 (VWR 02-0201-0500). Reactions were run on a thermocycler with the following settings:

344 1. 98°C for 30 sec

345 2. 30 PCR cycles:

346 (a) 98°C for 10 sec

347 (b) annealing temp. for 15 sec

348 (c) 72°C for 20 sec per kbp

349 3. 72°C for 2 min

350 4. 10°C hold

351 **Gibson cloning**

352 Gibson assembly was used to construct destination vectors, which were designed for
353 TypeIIS-based cloning. Reactions closely followed instructions from the NEBuilder HiFi DNA
354 Assembly Master Mix (NEB, E2621S). Fragments were amplified with PCR and designed to have
355 20-30 bp overlaps. The DpnI enzyme was used to digest template plasmid or *X. dendrorhous*

356 genomic DNA according to the manufacturer's instructions (NEB, R0176S). The amplified
357 fragments were purified using the Zymo Clean & Concentrator Kit (Zymo, D4005), followed by
358 dilution to 0.2 pmols for 2-3 fragments or 0.5 pmols for 4 or more fragments. The fragments, 10
359 µL of HiFi master mix, and nuclease free water were combined in a PCR tube for a 20 µL total
360 reaction volume. The mixture was run on a thermocycler at 50°C for 60 minutes, with a hold at
361 10°C.

362 **TypeIIS Cloning**

363 A modular, hierarchical TypeIIS cloning scheme was used construct genetic designs for
364 integration into *X. dendrorhous*. This scheme consisted of three levels; transcriptional parts (level
365 0), transcription units (level 1), and integrative pathways (level 2). Cloning reactions were based
366 on the enzymes BbsI (Thermo Scientific, ER1011) or BsaI (NEB, R3733). Cloning reactions
367 consisted of 1 µL of N parts, 1 µL of BsaI or BbsI, 1 µ L of 10X Ligase Buffer, 0.4 µL of T4 DNA
368 ligase (Promega, M1794), and 7.9 - N µL of nuclease free water, where N is the number of parts.
369 Reactions were run on a thermocycler at 37°C for 5 hours, 50 °C for 15 minutes, 80 °C for 20
370 minutes, and a hold at 10°C.

371 **Parts and strain design**

372 All genetic parts used in this study can be found in Supplementary Table 1.

373 **Minimum Inhibitory Concentration Assay**

374 *X. dendrorhous* cultures were diluted with YPD to an OD_{600} = 1.0 and 100 µL was pipetted
375 into columns 2-11 of a 96-well plate (Corning, 3596). Column 11 served as a positive control of
376 only X. dendrorhous culture. A negative control of 100 µL YPD was pipetted into column 12. The
377 antifungals hygromycin (ThermoFisher, 10687010), zeocin (Jena Bioscience, AB-103S),

378 geneticin (ThermoFisher, 10131-035), and nourseothricin (Jena Bioscience, AB-101L) were
379 chosen for the experiment. Stocks of each antifungal were made in concentrations of 5120 µg/mL
380 and 7680 µg/mL. Three replicates of antifungal concentration were made by pipetting 200 µL of
381 an antifungal into three wells of column 1. A multichannel pipette was used to perform a serial
382 dilution to column 10. At column 10, 100 µL of the culture and antibiotic mixture was pipetted and
383 discarded, leaving 100 µL of mixture in every well. The 96-well plates were incubated at 21°C for
384 3 days. The OD_{600} was measured on a BioTek Synergy H1 plate reader with column 12 as a
385 blank. Outliers were calculated using an interquartile range and were excluded in survival percent
386 calculations.

387 ***X. dendrorhous* transformation**

388 Integrative pathway DNA for transformation was excised from level 2 vectors with a BsaI
389 digestion. This digestion was comprised of 40 µL plasmid DNA, 5 µL 10X CutSmart Buffer, 2 µL
390 BsaI, and 3 µL nuclease free water. The reaction was run at 37°C for 10 hours, 80°C for 20
391 minutes, and a hold at 10°C. The resulting DNA fragments were then purified with the Zymo Clean
392 & Concentrator Kit and were ready for transformation. *X. dendrorhous* transformations were
393 based on an electroporation method described by Visser et. al.[34] *X. dendrorhous* was first
394 streaked on a YPD agar plate and grown at 21°C for approximately 2 days. A single colony was
395 used to inoculate 50 mL YPD media in a 125 mL Erlenmeyer flask. The cells were shaken at 21°C
396 and 200 rpm for another 2 days. These cells were then used to inoculate 200 mL of YPD in a 1 L
397 Erlenmeyer flask at OD_{600} = 0.02. The cells were grown at 21°C and 200 rpm until reaching OD_{600}
398 = 1.2 (approximately 20 hours). From here, the cells were pelleted at 1500 x g for 5 min and
399 resuspended in 25 mL of freshly made 50 mM potassium phosphate buffer (pH=7.0, Sigma-
400 Aldrich, P8281-100G & P9791-100G) with 25 mM diothiothreitol (Acros Organics, 426380500).
401 The cells were incubated at room temperature for 15 minutes, and then pelleted at 4°C for 5

402 minutes at 1500 x g. The cells were then washed with 25 mL of ice cold STM buffer (pH = 7.5,
403 270 mM sucrose, Millipore Sigma, 1.07651.5000, 10 mM Tris HCl, Alfa Aesar, J67233, 1 mM
404 $MgCl_2$, VWR, E525-100ML) and spun down again at 4°C for 5 minutes at 1500 x g. This wash
405 step was repeated and followed by resuspension of the pellet in 500 µL of STM buffer. Now
406 electrocompetent, the cells were divided into 60 µL aliquots and kept on ice until electroporation.
407 10 µL of transforming DNA was mixed with a 60 µL aliquot and transferred to an ice cold 0.2 cm
408 electroporation cuvette (ThermoFisher, 21-237-2). Electroporation was performed with a Gene
409 Pulser electroporator (Bio-Rad, 1998.018.1, 1998.018.2, & 1998.018.3) at 0.8 kV, 1000 ohms,
410 and 25 µF. Immediately following the electric pulse, 500 µL of ice cold YPD was added to the
411 cuvette. This mixture was then transferred to 4 mL of YPD in a 14 mL Falcon tube and grown
412 overnight on a rotating drum. The next morning, the cells were spun down for 5 minutes at 1500
413 x g, resuspended in 500 mL of filtered water, and spread onto selection plates. The plates were
414 incubated at 21°C until colonies appeared, which typically occurred in 2-3 days.

415

416 **Astaxanthin extraction from wild-type and *crtYB* knockouts**

417 *X. dendrorhous* CBS 6938 wild-type and *crtYB* knockout strains were grown for 3 days in
418 the dark at 21°C and 200 rpm. 1 mL of culture was taken forward and centrifuged at 10,850 x g
419 for 10 minutes. The cell pellet was washed with Milli-Q filtered water twice before resuspension
420 in 1 mL of acetone (SigmaAldrich, 34850-1L). Cell and acetone mixtures were poured into pre-
421 filled tubes of 400-micron zirconium beads (OPS Diagnostics, PFMB 400-100-34), then
422 transferred to snap-cap microcentrifuge tubes (Eppendorf, 022363743). The Bullet Blender Storm
423 Pro tissue homogenizer (NextAdvance, BT24M) was used at 12 m/s for 5 minutes to mechanically
424 lyse the cells. Afterward, tubes were centrifuged for 10,850 x g for 10 minutes. 200 µL of
425 supernatant was pipetted into a nylon syringeless filter (Whatman, UN203NPENYL) and

426 transferred to a 2 mL chromatography vial (Agilent, 5181-3376) with a glass vial insert (5183-
427 2085) and crimp top cap (Agilent, 8010-0051).

428

429 **Ultra-high performance liquid chromatography detection of astaxanthin**

430 UPLC analysis was performed using a modified method from Bohoyo-Gil et al.[35]
431 Modifications include an injection volume of 10 µL, usage of a Shimadzu Nexcol C18 1.8 µm
432 column (Shimadzu, 220-91394-03), and analysis on the Nexera Series UPLC (Shimadzu; RF-
433 20AXS, RID-20A, SCL-40, DGU-403, DGU-405, CTO-40C, SPD-M40, C-40 LPGE, LC-40D XS,
434 SIL-40C XS).

435 **Bioluminescence detection assay**

436 LPA cultures were started in 2 mL of YPD media at OD_{600} = 1 and shaken for 24 hours at
437 200 rpm. *X. dendrorhous* was exposed to either a UV (λ = 400 nm) or dark (no LED light) condition.
438 Bioluminescence was detected using the Nano-Glo Luciferase Assay System (Promega, N1110).
439 Assay buffer and assay reagent were mixed in a 50:1 ratio to create to assay solution. Aliquots of
440 50 µL of *X. dendrorhous* cells were mixed with 50 µL assay solution in a 96-well plate (Corning,
441 3904). Bioluminescence was measured on a BioTek Synergy H1 plate reader.

FUNDING

This project is supported by a National Science Foundation CAREER award to EMY, award number 1944046. EET is supported by a National Science Foundation Graduate Research Fellowship.

The work (proposal 10.46936/10.25585/60001246) conducted by the U.S. Department of Energy Joint Genome Institute (https://ror.org/04xm1d337), a DOE Office of Science User Facility, is supported by the Office of Science of the U.S. The Department of Energy operated under Contract No. DE-AC02-05CH11231.

Development of Prymetime was supported by the Office of the Director of National Intelligence (ODNI), Intelligence Advanced Research Projects Activity (IARPA) under Finding Engineering Linked Indicators (FELIX) program contract #N66001-18-C-4507. The views and conclusions contained herein are those of the authors and should not be interpreted as necessarily representing the official policies, either expressed or implied, of ODNI, IARPA, or the U.S. Government. The U.S. Government is authorized to reproduce and distribute reprints for governmental purposes notwithstanding any copyright annotation therein.

AUTHOR CONTRIBUTIONS

EET, JHC, and EMY conceived of the study. EET and JHC performed all experiments and analysis save the sequencing and initial processing of RNA-seq data. CBM and GTN constructed the light plate apparatus (LPA). KM acquired microscope images of red yeast. AL, SM, and IG performed transcriptomic sequencing and initial processing of RNA-seq data. EET and EMY wrote the manuscript.

[*] Emma E. Tobin and Joseph H. Collins contributed equally.

CONFLICT OF INTEREST

The authors declare that there are no conflicts of interest regarding this research study.

460 **FIGURES**

461

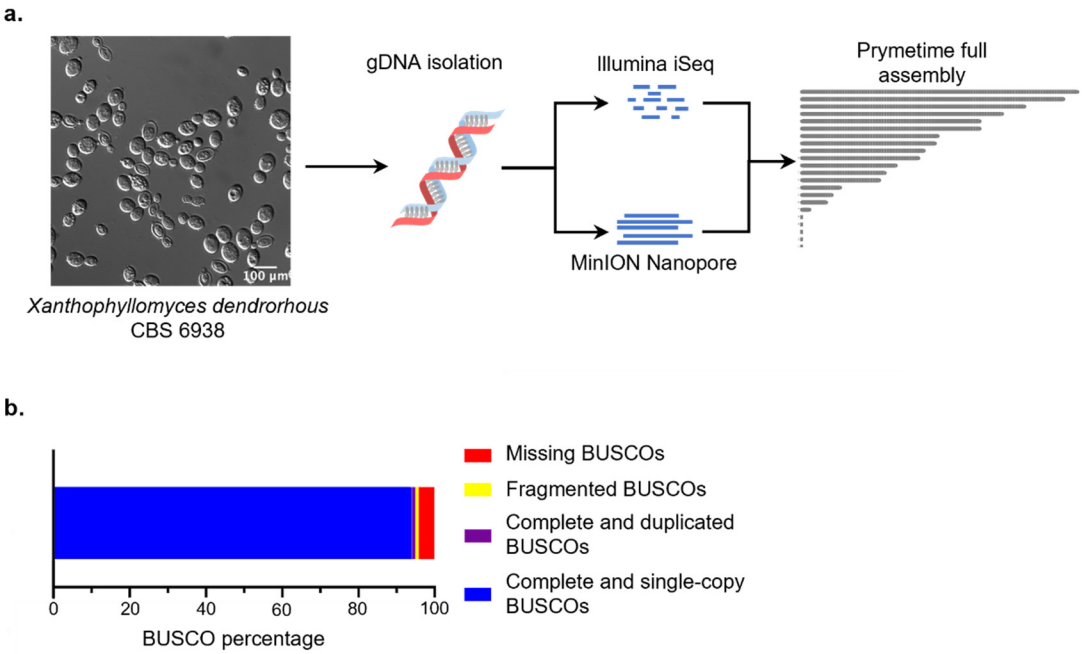

462 Figure 1. **Overview of *X. dendrorhous* genome sequencing and quality analysis. (a)**
463 schematic of Prymetime next generation sequencing workflow. Illumina and Nanopore reads are
464 combined for a higher quality genome. **(b)** BUSCO analysis of the *X. dendrorhous* genome.

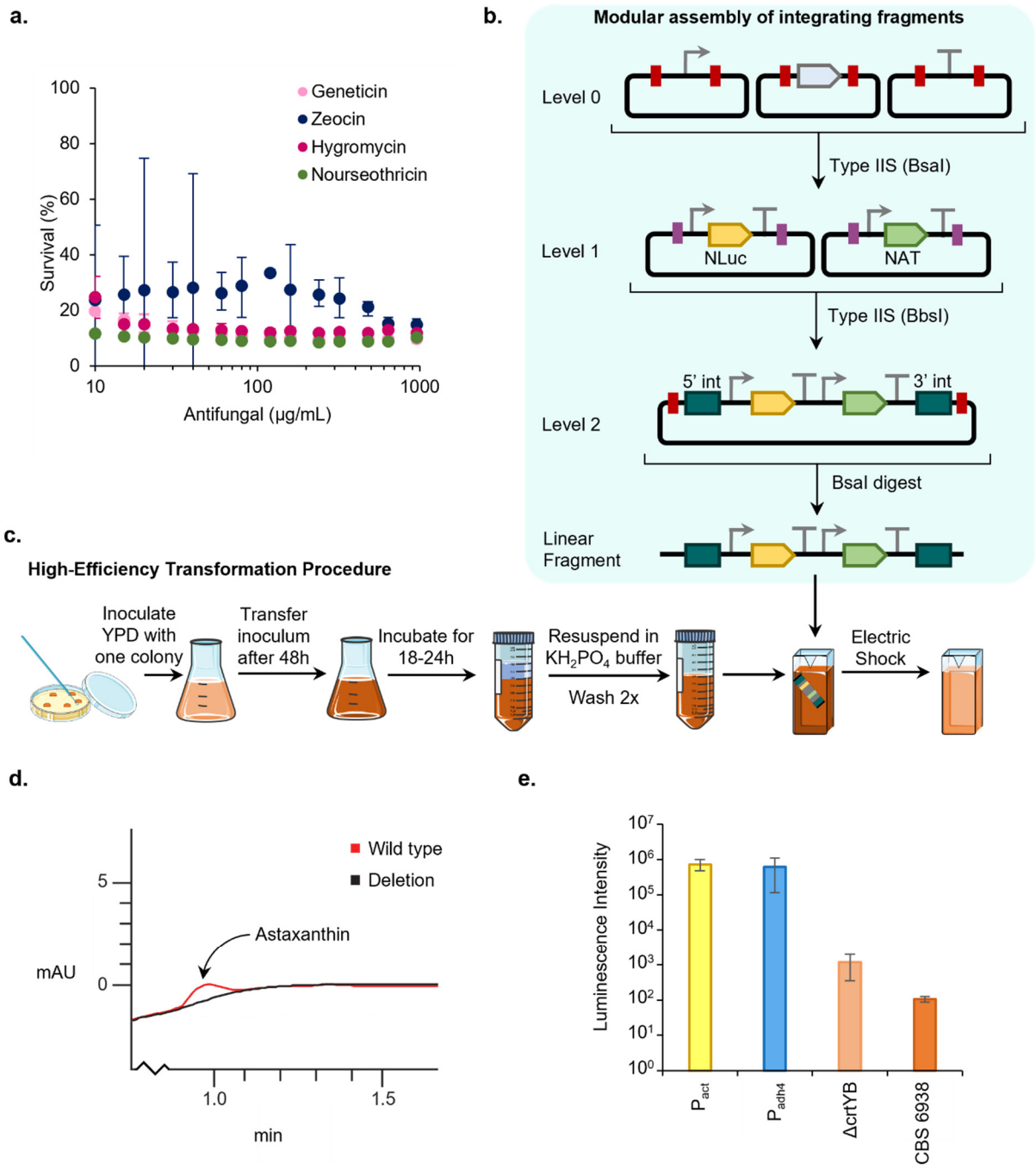

Figure 2. **"Onboarding" process of *X. dendrorhous*. (a)** Minimum inhibitory concentration assay data from testing geneticin, zeocin, hygromycin, and nourseothricin against *X. dendrorhous*. **(b)** Cloning workflow adapted from CIDAR for homologous recombination into the *crtYB* site. **(c)** Depiction of high-efficiency transformation procedure. **(d)** Overlapped chromatograms illustrating the lack of astaxanthin at a retention time of 0.998. Wild type is shown in red and the *crtYB* knockout is shown in black. **(e)** Comparison of luminescence between two strong constitutive promoters for *act* and *adh4,* the *crtYb* knockout, and CBS 6938 wild type.

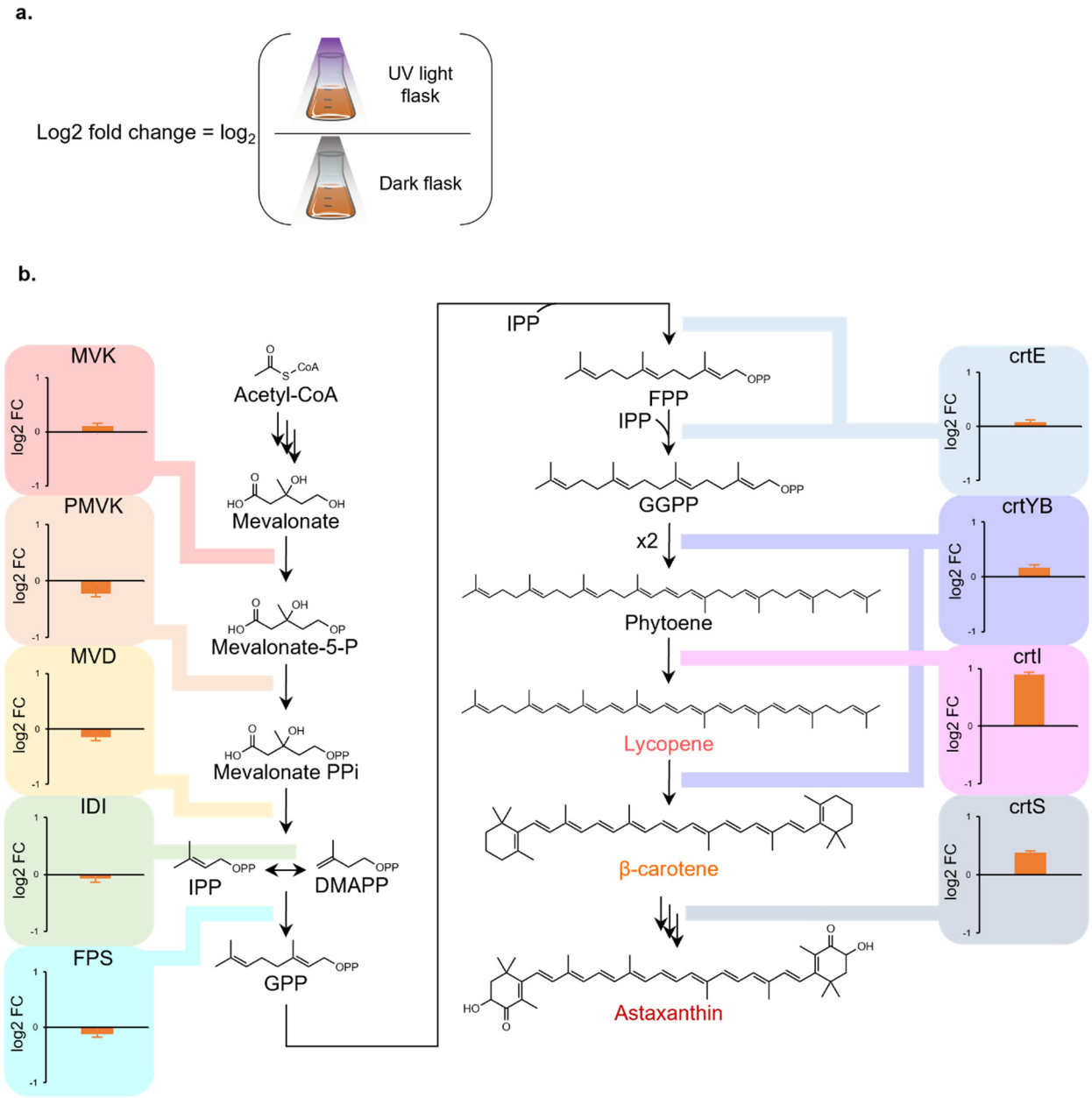

Figure 3. **Preliminary investigation into ultraviolet light regulation through RT-qPCR. (a)** RT-qPCR results for enzymatic steps in the mevalonate and carotenogenesis pathway. Upstream steps are not affected by UV exposure, but downstream genes *crtYB*, *crtI*, and *crtS* are considerably induced. **(b)** RNA isolation process for transcriptomic sequencing. Six treatments were implemented including four light wavelengths, a positive control (H_2O_2), and a negative control (dark).

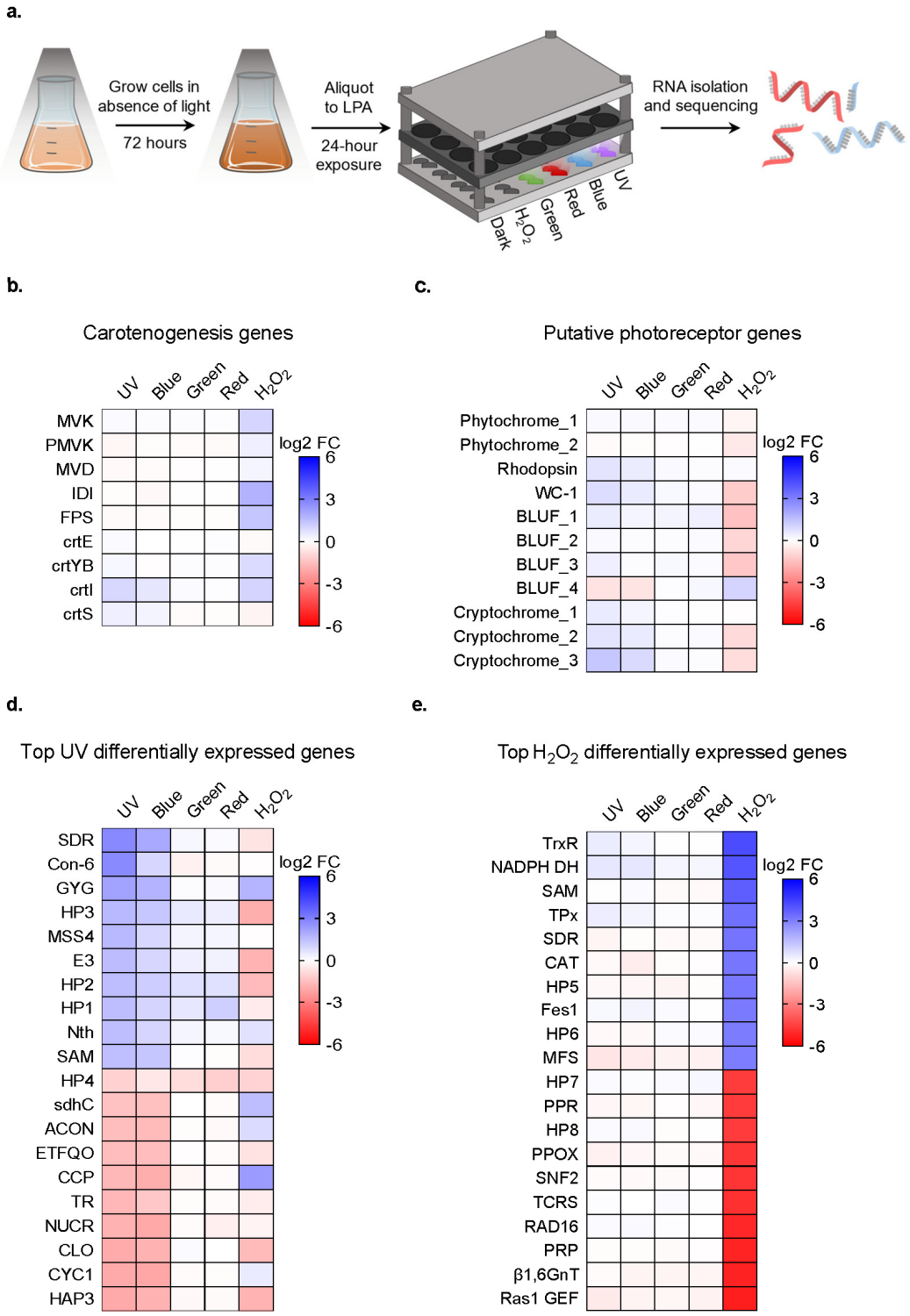

Figure 4. **Heatmaps illustrating the response of gene expression to various light treatments and a general oxidative stressor, H_2O_2. Blue represents induction and red represents repression. (a)** Regulation of mevalonate and carotenogenesis genes by light and H_2O_2. **(b)** Regulation of putative photoreceptors. Numbers are arbitrarily assigned. **(c)** Top ten UV induced and repressed genes. **(d)** Top ten H_2O_2 induced and repressed genes.

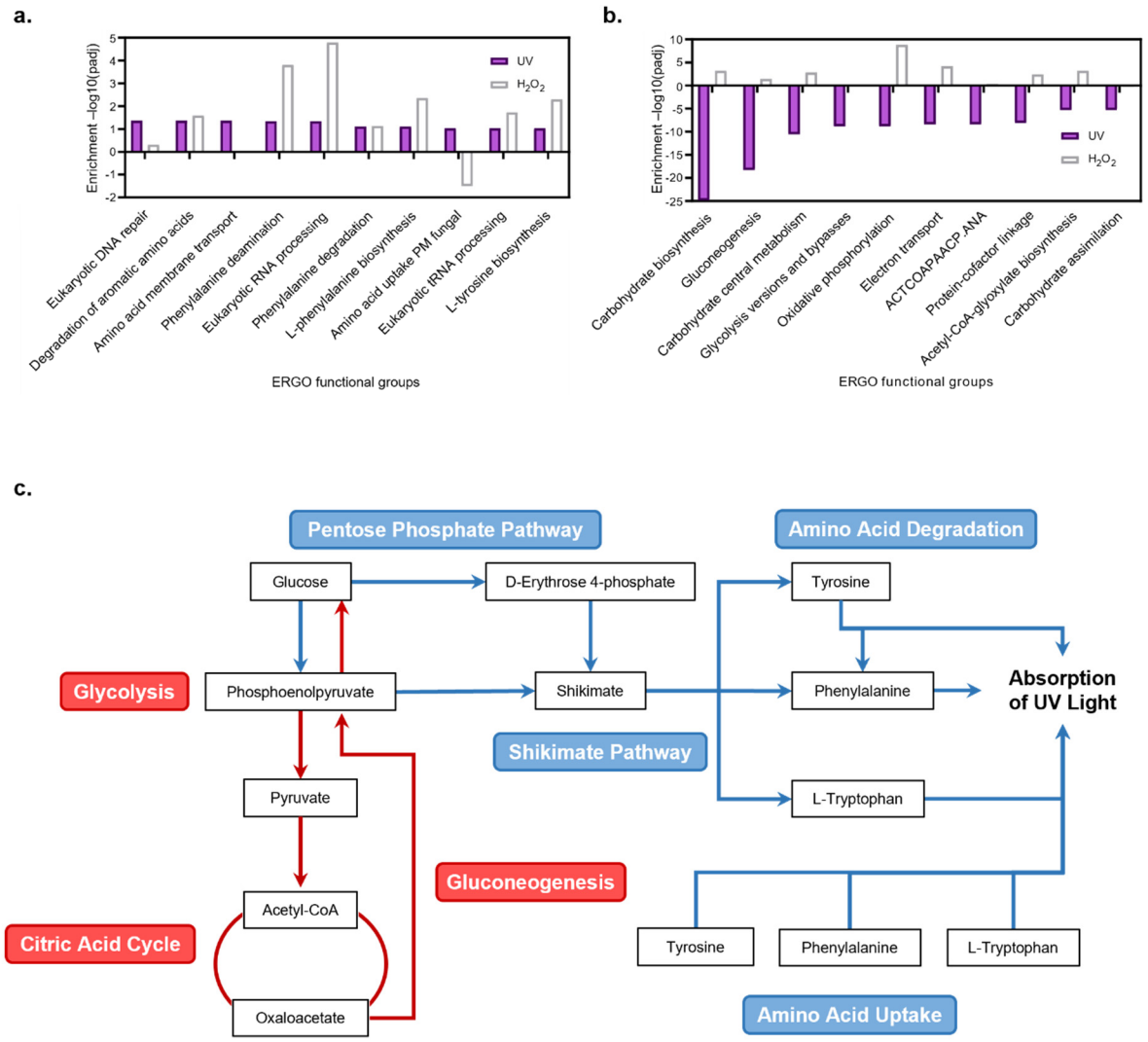

Figure 5. **Transcriptomic analyses clustered by ERGO functional groups, and therefore metabolic processes. (a)** Overall up- and downregulation of metabolic processes by UV light or H_2O_2. **(b)** Summary of metabolic processes regulated by UV light. Generally, metabolic flux is being drawn from central carbon metabolism to synthesis of aromatic amino acids.

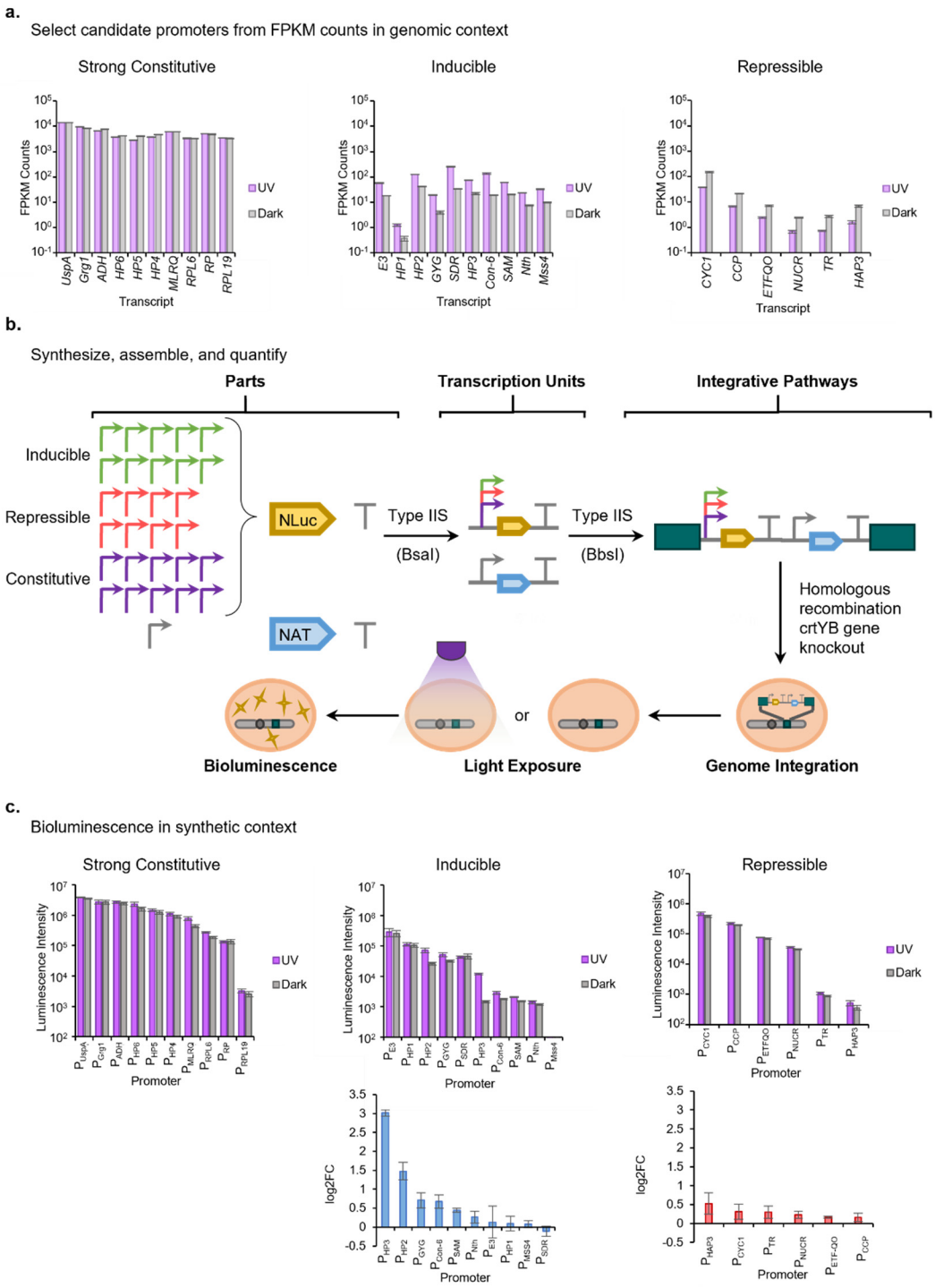

Figure 6. **Comparison of transcriptome-derived promoters to predicted expression through FPKM values. (a)** Putative **c**onsitutive promoters are shown. **(b)** Putative nducible promoters are shown. **(c)** Putative epressible promoters are shown. **(d)** Depiction of putative inducible promoters with log2 fold-change. P_{HP3} has the greatest induction to UV light at a log2 fold-change of 3.01. **(e)** Depiction of putative repressible promoters with log2 fold-change. None were found to be repressible.

499 **REFERENCES**

500 (1) Boekhout, T.; Amend, A. S.; El Baidouri, F.; Gabaldón, T.; Geml, J.; Mittelbach, M.; Robert,
501 V.; Tan, C. S.; Turchetti, B.; Vu, D.; Wang, Q. M.; Yurkov, A. Trends in Yeast Diversity
502 Discovery. *Fungal Diversity*. 2022. https://doi.org/10.1007/s13225-021-00494-6.

503 (2) Wagner, J. M.; Alper, H. S. Synthetic Biology and Molecular Genetics in Non-Conventional
504 Yeasts: Current Tools and Future Advances. *Fungal Genetics and Biology* **2016**, *89*.
505 https://doi.org/10.1016/j.fgb.2015.12.001.

506 (3) Bellora, N.; Moliné, M.; David-Palma, M.; Coelho, M. A.; Hittinger, C. T.; Sampaio, J. P.;
507 Gonçalves, P.; Libkind, D. Comparative Genomics Provides New Insights into the Diversity,
508 Physiology, and Sexuality of the Only Industrially Exploited Tremellomycete: Phaffia
509 Rhodozyma. *BMC Genomics* **2016**, *17* (1). https://doi.org/10.1186/s12864-016-3244-7.

510 (4) Nielsen, J. Yeast Systems Biology: Model Organism and Cell Factory. *Biotechnology*
511 *Journal*. 2019. https://doi.org/10.1002/biot.201800421.

512 (5) Li, W.; Cui, L.; Mai, J.; Shi, T. Q.; Lin, L.; Zhang, Z. G.; Ledesma-Amaro, R.; Dong, W.; Ji,
513 X. J. Advances in Metabolic Engineering Paving the Way for the Efficient Biosynthesis of
514 Terpenes in Yeasts. *Journal of Agricultural and Food Chemistry*. 2022.
515 https://doi.org/10.1021/acs.jafc.2c03917.

516 (6) Torres-Haro, A.; Verdín, J.; Kirchmayr, M. R.; Arellano-Plaza, M. Metabolic Engineering for
517 High Yield Synthesis of Astaxanthin in Xanthophyllomyces Dendrorhous. *Microbial Cell*
518 *Factories*. 2021. https://doi.org/10.1186/s12934-021-01664-6.

519 (7) Rodríguez-Sáiz, M.; De La Fuente, J. L.; Barredo, J. L. Xanthophyllomyces Dendrorhous
520 for the Industrial Production of Astaxanthin. *Applied Microbiology and Biotechnology*. 2010.
521 https://doi.org/10.1007/s00253-010-2814-x.

522 (8) Tropea, A.; Gervasi, T.; Melito, M. R.; Curto, A. Lo; Curto, R. Lo. Does the Light Influence
523 Astaxanthin Production in Xanthophyllomyces Dendrorhous? *Nat Prod Res* **2013**, *27* (7).
524 https://doi.org/10.1080/14786419.2012.688045.

525 (9) Vázquez, M. Effect of the Light on Carotenoid Profiles of Xanthophyllomyces Dendrorhous
526 Strains (Formerly Phaffia Rhodozyma). *Food Technol Biotechnol* **2001**, *39* (2).

527 (10) Collins, J. H.; Keating, K. W.; Jones, T. R.; Balaji, S.; Marsan, C. B.; Çomo, M.; Newlon, Z.
528 J.; Mitchell, T.; Bartley, B.; Adler, A.; Roehner, N.; Young, E. M. Engineered Yeast
529 Genomes Accurately Assembled from Pure and Mixed Samples. *Nat Commun* **2021**, *12*
530 (1). https://doi.org/10.1038/s41467-021-21656-9.

531 (11) Mülleder, M.; Capuano, F.; Pir, P.; Christen, S.; Sauer, U.; Oliver, S. G.; Ralser, M. A
532 Prototrophic Deletion Mutant Collection for Yeast Metabolomics and Systems Biology.
533 *Nature Biotechnology*. 2012. https://doi.org/10.1038/nbt.2442.

534 (12) Iverson, S. V.; Haddock, T. L.; Beal, J.; Densmore, D. M. CIDAR MoClo: Improved MoClo
535 Assembly Standard and New E. Coli Part Library Enable Rapid Combinatorial Design for
536 Synthetic and Traditional Biology. *ACS Synth Biol* **2016**, *5* (1).
537 https://doi.org/10.1021/acssynbio.5b00124.

538 (13) England, C. G.; Ehlerding, E. B.; Cai, W. NanoLuc: A Small Luciferase Is Brightening Up
539 the Field of Bioluminescence. *Bioconjugate Chemistry*. American Chemical Society May
540 18, 2016, pp 1175–1187. https://doi.org/10.1021/acs.bioconjchem.6b00112.

541 (14) Bereta, M.; Teplan, M.; Chafai, D. E.; Radil, R.; Cifra, M. Biological Autoluminescence as
542 a Noninvasive Monitoring Tool for Chemical and Physical Modulation of Oxidation in Yeast
543 Cell Culture. *Sci Rep* **2021**, *11* (1). https://doi.org/10.1038/s41598-020-79668-2.

544 (15) Shin, J.; South, E. J.; Dunlop, M. J. Transcriptional Tuning of Mevalonate Pathway
545 Enzymes to Identify the Impact on Limonene Production in Escherichia Coli. *ACS Omega*
546 **2022**, *7* (22). https://doi.org/10.1021/acsomega.2c00483.

547 (16) Yu, Z.; Fischer, R. Light Sensing and Responses in Fungi. *Nature Reviews Microbiology*.
548 2019. https://doi.org/10.1038/s41579-018-0109-x.

549 (17) Desrivières, S.; Cooke, F. T.; Parker, P. J.; Hall, M. N. MSS4, a Phosphatidylinositol-4-
550 Phosphate 5-Kinase Required for Organization of the Actin Cytoskeleton in
551 Saccharomyces Cerevisiae. *Journal of Biological Chemistry* **1998**, *273* (25), 15787–15793.
552 https://doi.org/10.1074/jbc.273.25.15787.

553 (18) Serafini, D. M.; Schellhorn, H. E. Endonuclease III and Endonuclease IV Protect
554 Escherichia Coli from the Lethal and Mutagenic Effects of Near-UV Irradiation. *Can J*
555 *Microbiol* **1999**, *45* (7). https://doi.org/10.1139/cjm-45-7-632.

556 (19) Bruchez, J. J. P.; Eberle, J.; Kohler, W.; Kruft, V.; Radford, A.; Russo, V. E. A. Bli-4, a Gene
557 That Is Rapidly Induced by Blue Light, Encodes a Novel Mitochondrial, Short Chain Alcohol
558 Dehydrogenase-like Protein in Neurospora Crassa. *Molecular and General Genetics* **1996**,
559 *252* (3). https://doi.org/10.1007/BF02173767.

560 (20) Sinha, R. P.; Häder, D. P. UV-Induced DNA Damage and Repair: A Review. *Photochemical*
561 *and Photobiological Sciences* **2002**, *1* (4), 225–236. https://doi.org/10.1039/b201230h.

562 (21) Olmedo, M.; Ruger-Herreros, C.; Luque, E. M.; Corrochano, L. M. A Complex
563 Photoreceptor System Mediates the Regulation by Light of the Conidiation Genes Con-10
564 and Con-6 in Neurospora Crassa. *Fungal Genetics and Biology* **2010**, *47* (4), 352–363.
565 https://doi.org/10.1016/j.fgb.2009.11.004.

566 (22) Llewellyn, C. A.; Greig, C.; Silkina, A.; Kultschar, B.; Hitchings, M. D.; Farnham, G.
567 Mycosporine-like Amino Acid and Aromatic Amino Acid Transcriptome Response to UV

568 and Far-Red Light in the Cyanobacterium Chlorogloeopsis Fritschii PCC 6912. *Sci Rep*
569 **2020**, *10* (1). https://doi.org/10.1038/s41598-020-77402-6.

570 (23) Gilchrest, B. A.; Park, H. Y.; Eller, M. S.; Yaar, M. Echanisms of Ultraviolet Light-Induced
571 Pigmentation. *Photochemistry and Photobiology*. American Society for Photobiology 1996,
572 pp 1–10. https://doi.org/10.1111/j.1751-1097.1996.tb02988.x.

573 (24) Bhatia, S.; Garg, A.; Sharma, K.; Kumar, S.; Sharma, A.; Purohit, A. P. Mycosporine and
574 Mycosporine-like Amino Acids: A Paramount Tool against Ultra Violet Irradiation.
575 *Pharmacognosy Reviews*. 2011. https://doi.org/10.4103/0973-7847.91107.

576 (25) Schwartz, C.; Shabbir-Hussain, M.; Frogue, K.; Blenner, M.; Wheeldon, I. Standardized
577 Markerless Gene Integration for Pathway Engineering in Yarrowia Lipolytica. *ACS Synth*
578 *Biol* **2017**, *6* (3). https://doi.org/10.1021/acssynbio.6b00285.

579 (26) Schwarzhans, J. P.; Wibberg, D.; Winkler, A.; Luttermann, T.; Kalinowski, J.; Friehs, K.
580 Non-Canonical Integration Events in Pichia Pastoris Encountered during Standard
581 Transformation Analysed with Genome Sequencing. *Sci Rep* **2016**, *6*.
582 https://doi.org/10.1038/srep38952.

583 (27) Gerhardt, K. P.; Olson, E. J.; Castillo-Hair, S. M.; Hartsough, L. A.; Landry, B. P.; Ekness,
584 F.; Yokoo, R.; Gomez, E. J.; Ramakrishnan, P.; Suh, J.; Savage, D. F.; Tabor, J. J. An
585 Open-Hardware Platform for Optogenetics and Photobiology. *Sci Rep* **2016**, *6*.
586 https://doi.org/10.1038/srep35363.

587 (28) Clum, A.; Huntemann, M.; Bushnell, B.; Foster, B.; Foster, B.; Roux, S.; Hajek, P. P.;
588 Varghese, N.; Mukherjee, S.; Reddy, T. B. K.; Daum, C.; Yoshinaga, Y.; O'Malley, R.;
589 Seshadri, R.; Kyrpides, N. C.; Eloe-Fadrosh, E. A.; Chen, I.-M. A.; Copeland, A.; Ivanova,
590 N. N. DOE JGI Metagenome Workflow. *mSystems* **2021**, *6* (3).
591 https://doi.org/10.1128/msystems.00804-20.

592 (29) Kim, D.; Langmead, B.; Salzberg, S. L. HISAT: A Fast Spliced Aligner with Low Memory
593 Requirements. *Nat Methods* **2015**, *12* (4). https://doi.org/10.1038/nmeth.3317.

594 (30) Liao, Y.; Smyth, G. K.; Shi, W. FeatureCounts: An Efficient General Purpose Program for
595 Assigning Sequence Reads to Genomic Features. *Bioinformatics* **2014**, *30* (7).
596 https://doi.org/10.1093/bioinformatics/btt656.

597 (31) Love, M. I.; Huber, W.; Anders, S. Moderated Estimation of Fold Change and Dispersion
598 for RNA-Seq Data with DESeq2. *Genome Biol* **2014**, *15* (12).
599 https://doi.org/10.1186/s13059-014-0550-8.

600 (32) Overbeek, R.; Larsen, N.; Walunas, T.; D' Souza, M.; Pusch, G.; Selkov, E.; Liolios, K.;
601 Joukov, V.; Kaznadzey, D.; Anderson, I.; Bhattacharyya, A.; Burd, H.; Gardner, W.; Hanke,
602 P.; Kapatral, V.; Mikhailova, N.; Vasieva, O.; Osterman, A.; Vonstein, V.; Fonstein, M.;
603 Ivanova, N.; Kyrpides, N. The ErgoTM Genome Analysis and Discovery System. *Nucleic*
604 *Acids Research*. 2003. https://doi.org/10.1093/nar/gkg148.

605 (33) Luo, W.; Friedman, M. S.; Shedden, K.; Hankenson, K. D.; Woolf, P. J. GAGE: Generally
606 Applicable Gene Set Enrichment for Pathway Analysis. *BMC Bioinformatics* **2009**, *10*.
607 https://doi.org/10.1186/1471-2105-10-161.

608 (34) Visser, H.; Van Ooyen, A. J. J.; Verdoes, J. C. Metabolic Engineering of the Astaxanthin-
609 Biosynthetic Pathway of Xanthophyllomyces Dendrorhous. *FEMS Yeast Research*. 2003.
610 https://doi.org/10.1016/S1567-1356(03)00158-2.

611 (35) Bohoyo-Gil, D.; Dominguez-Valhondo, D.; García-Parra, J. J.; González-Gómez, D.
612 UHPLC as a Suitable Methodology for the Analysis of Carotenoids in Food Matrix.
613 *European Food Research and Technology* **2012**, *235* (6). https://doi.org/10.1007/s00217-
614 012-1838-0.

615